Journal of Proteomics 155 (2017) 85–98

Contents lists available at ScienceDirect

Journal of Proteomics

journal homepage: www.elsevier.com/locate/jprot

Integration of proteomics and metabolomics to elucidate metabolic adaptation in *Leishmania*

Snezhana Akpunarlieva [a], Stefan Weidt [a], Dhilia Lamasudin [b], Christina Naula [a], David Henderson [a], Michael Barrett [a], Karl Burgess [a], Richard Burchmore [a,*]

[a] Institute of Infection, Immunity and Inflammation and Glasgow Polyomics, College of Medical, Veterinary & Life Sciences, University of Glasgow, UK
[b] Department of Cell & Molecular Biology, Faculty of Biotechnology & Biomolecular Sciences, University Putra Malaysia, Malaysia

ARTICLE INFO

Article history:
Received 10 August 2016
Received in revised form 13 December 2016
Accepted 16 December 2016
Available online 29 December 2016

Keywords:
Leishmania
Glucose transporter null mutant
Metabolic adaptation
Proteomics
Metabolomics
Data integration

ABSTRACT

Leishmania parasites multiply and develop in the gut of a sand fly vector in order to be transmitted to a vertebrate host. During this process they encounter and exploit various nutrients, including sugars, and amino and fatty acids. We have previously generated a mutant *Leishmania* line that is deficient in glucose transport and which displays some biologically important phenotypic changes such as reduced growth in axenic culture, reduced biosynthesis of hexose-containing virulence factors, increased sensitivity to oxidative stress, and dramatically reduced parasite burden in both insect vector and macrophage host cells. Here we report the generation and integration of proteomic and metabolomic approaches to identify molecular changes that may explain these phenotypes. Our data suggest changes in pathways of glycoconjugate production and redox homeostasis, which likely represent adaptations to the loss of sugar uptake capacity and explain the reduced virulence of this mutant in sand flies and mammals. Our data contribute to understanding the mechanisms of metabolic adaptation in *Leishmania* and illustrate the power of integrated proteomic and metabolomic approaches to relate biochemistry to phenotype.

Biological significance: This paper reports the application of comparative proteomic and metabolomic approaches to reveal the molecular basis for important phenotypic changes *Leishmania* parasites that are deficient in glucose uptake. *Leishmania* cause a very significant disease burden across the world and there are few effective drugs available for control. This work shows that proteomics and metabolomics can produce complementary data that advance understanding of parasite metabolism and highlight potential new targets for chemotherapy.

1. Introduction

Pathogenic protozoa of the genus *Leishmania* encounter high levels of glucose and other sugars as they develop within the alimentary tract of the sand fly vector and they can exploit these carbohydrates as a source of energy and carbon [1,2]. Upon transmission to the mammalian host, where they are obligate intracellular parasites of macrophages, *Leishmania* proliferate in conditions where glucose and other energy-providing carbohydrates may be sparse [3]. *Leishmania* can thrive on alternative energy sources, such as amino acids and fatty acids [4], and such substrates may be important during phases of the life cycle when sugars are depleted. *Leishmania*, nonetheless, utilize glucose when available and maintain a carbohydrate reserve in the form of β-mannan [5]. When glucose is scarce, *Leishmania* can mobilize mannan reserves or invoke gluconeogenesis to generate sugar phosphates for anabolic pathways and to maintain β-mannan [6]. In the macrophage host cell, *Leishmania* elaborate a stringent response that results in more efficient utilization of energy substrates [7].

The promastigote form of *Leishmania*, which is adapted to life in the insect vector, accumulates glucose robustly [8] but can be cultured in medium that lacks sugars. The *L. mexicana* transporters (LmGT) that are responsible for glucose uptake have been identified and characterized [9], and a glucose transporter knockout line (*ΔLmGT*) has been generated [10]. *ΔLmGT* promastigotes do not accumulate glucose but multiply with similar kinetics to wild type parasites cultured in media that is glucose-free but amino acid replete. However, *ΔLmGT* parasites are very significantly compromised in their ability to infect both the sand fly vector and mammalian macrophage, suggesting that glucose uptake is important for parasite virulence.

In addition to reduced virulence, *ΔLmGT Leishmania* exhibit a number of specific phenotypic changes. *ΔLmGT* cells multiply more slowly and are significantly smaller [11] than wild type *L. mexicana* promastigotes, when maintained in a glucose-replete culture medium. However, when wild type and *ΔLmGT* lines are propagated in a glucose-depleted medium, growth rate and cell volume are similar [10],

* Corresponding author.
E-mail address: richard.burchmore@glasgow.ac.uk (R. Burchmore).

http://dx.doi.org/10.1016/j.jprot.2016.12.009

suggesting that these phenotypes are the simple consequence of an inability to exploit glucose in the culture environment. *ΔLmGT* parasites are also significantly more sensitive to oxidative stress and to nutrient deprivation [11], phenotypes that likely contribute to their reduced virulence in both hosts. *ΔLmGT* is able to synthesize carbohydrate via the gluconeogenic pathway, which appears to be constitutively active in this mutant [12]. Nonetheless, the production of glycoconjugates and energy storage carbohydrates, both important virulence factors, is significantly reduced compared with wild type parasites, in which gluconeogenesis does not operate when environmental glucose levels are high. While expression of a functional glucose transporter leads to the reversion of many of these phenotypes [10,12,13], metabolic changes compensate only partially for the inability of *ΔLmGT Leishmania* to acquire exogenous glucose, access to which appears to be essential in the clinically relevant amastigote stage. This underscores the importance of glucose transport to the parasite and the potential of glucose transport inhibitors as *anti*-parasitic drugs necessitates understanding how *Leishmania* can adapt to circumvent lesions in nutrient acquisition.

To address this, we have taken comparative proteomic and metabolomic approaches to identify proteins and metabolites that show altered abundance in *ΔLmGT Leishmania*. A number of robust and reproducible changes have been observed and modulated proteins and metabolites have been identified in pathways that are central to glucose anabolism and response to oxidative stress. We have also observed a very significant modulation in a key component of the *Leishmania* flagellum.

2. Experimental procedures

2.1. Global proteomic analysis

Wild type and *ΔLmGT L. mexicana* promastigotes were grown at 25 °C in a hemoflagellate-modified minimum essential medium, HOMEM [14] (Gibco, Thermo Fisher Scientific), supplemented with 10% heat-inactivated fetal calf serum (iFCS) and subjected to a multiplex 2-dimensional difference gel electrophoresis (2D DiGE) analysis [15]. Four independent replicate lysates were prepared for each line and analysed as pairs by 2D gel electrophoresis. A pooled standard sample, comprising equal amounts of every lysate was included on each of these gels, to facilitate matching of replicate gels and to enable intra-gel normalization of spot intensities. In parallel to the analytical DiGE gels, a preparative gel was loaded with 500 μg of the pooled standard sample and stained for protein. Spot detection was performed for each gel image using Decyder software, with no exclusion criteria. After spot matching with extensive manual "land-marking", approximately 2000 spots were confidently matched in all 12 DiGE spot maps. Decyder Batch Variance Analysis (BVA) was used to highlight those spots that showed reproducible modulation of expression ($p \leq 0.05$; $n = 4$). Spots of interest were cut from the stained preparative gel, digested in-gel with trypsin and analysed by mass spectrometry (MS). Protein identification was performed using the Mascot search engine to interrogate the *Leishmania mexicana* genome sequence dataset.

2.2. 2D DiGE analysis

Sample preparation, 2D gel electrophoresis, gel scanning and analysis, spot cutting and generation of tryptic peptide were performed as previously described [16].

2.3. Peptide analysis by mass spectrometry

Peptides were solubilized in 2% acetonitrile (ACN) (Thermo Fisher Scientific) with 0.1% formic acid (FA) (Sigma-Aldrich) and fractionated on a nanoflow ultra-high performance liquid chromatography (UHPLC) system (Thermo Fisher Scientific) before online analysis by electrospray ionisation (ESI) mass spectrometry on an Amazon Speed ion trap MS/MS (Bruker). Peptides were desalted and concentrated for 4 min on a C18 trap column, then separated on a Pepmap C18 reversed phase column (LC Packings) by elution with an ACN gradient (in 0.1% *v*/v FA) (3.2–32% *v*/v 4–27 min, 32% to 80% *v*/v 27–36 min, held at 80% *v*/v 36–41 min and re-equilibrated at 3.2%) for a total time of 45 min. A fixed solvent flow rate of 0.3 μl/min was used for the analytical column. The trap column solvent flow rate was fixed at 25 μl/min, using 2% ACN with 0.1% *v*/v FA. MS analysis was performed using a continuous duty cycle of survey MS scan followed by up to ten MS/MS analyses of the most abundant peptides, choosing the most intense multiply charged ions with dynamic exclusion for 120 s.

MS data were processed using Data Analysis software (Bruker) and the automated Matrix Science Mascot Daemon server (v2.4.1). Protein identifications were assigned using the Mascot search engine to interrogate protein sequences in the *Leishmania mexicana* genome sequence dataset, 30-06-2012 release, obtained from TriTrypDB.org, allowing a mass tolerance of 0.4 Da for both MS and MS/MS analyses.

2.4. Global untargeted metabolomic analysis

Wild type and *ΔLmGT* promastigotes were grown at 27 °C in HOMEM supplemented with 10% heat-inactivated fetal bovine serum (iFBS) (PAA Laboratories) and subjected to a metabolite extraction according to a previously described method [17]. Briefly, triplicate wild type and *ΔLmGT* cell cultures, each containing 3.0×10^8 cells in total, were rapidly quenched to 4 °C by immersion in dry ice/ethanol bath (Fig. 1). The quenched cells were harvested and washed twice with 10 ml of phosphate buffer saline (PBS) (Sigma-Aldrich) by centrifugation at 1000 ×*g* for 10 min at 4 °C. Washed cell pellets and 10 μl of spent media were subjected to chloroform/methanol/water (1:3:1, *v*/v/v) extraction by shaking the mixtures for 1.5 h at 4 °C. Metabolite extracts were separated on a 4.6 mm × 150 mm zwitterionic-polymeric hydrophilic interaction chromatography (ZIC-pHILIC) column (SeQuant). The gradient, at a flow rate of 300 μl/min, was 80–20% 80% ACN in 0.08% FA over 30 min, 5% 80% ACN in 0.08% FA over 10 min, and 80% 80% ACN in 0.08% FA over 6 min. The spray voltage, capillary temperature and maximum spray current were 3.5–4.5 kV, 275 °C and 100, respectively. Samples were analysed on an Orbitrap Exactive mass spectrometer (Thermo Fisher Scientific) operating in alternating positive and negative modes with a mass range of 70–1400 amu. Raw MS data were analysed with IDEOM using the default parameters [18]. Metabolite identification was based on accurate mass and predicted retention time. Retention times of 239 compounds were verified against unambiguous standard mixes.

2.5. Targeted carbohydrate analysis

Wild type and *ΔLmGT* promastigotes were grown at 27 °C in HOMEM supplemented with 10% iFBS and subjected to chloroform/methanol/water extraction as described above. 100 μl of the fresh media (HOMEM supplemented with 10% iFBS), wild type and *ΔLmGT* promastigote lysates, and spent cell culture media were transferred into 9 mm screw cap borosilicate glass 1.5 ml tapered vials (VWR). 1 nmol of ^{13}C-D-glucose was added to each aliquoted sample. Samples were dried in a ReactiVap (Thermo Fisher Scientific), with a gentle nitrogen stream at 60 °C for 30 min. 10 μl of 40 mg/ml (*w*/*v*) methoxyamine-HCl (Sigma-Aldrich) in pyridine (Sigma-Aldrich) was added to each dried vial, vortexed for 30 s and incubated at 60 °C for 120 min. Following the methoximation step, 90 μl of *N*-methyl-N-(trimethylsilyl) trifluoroacetamide (MSTFA) (Thermo Fisher Scientific) plus 1% trimethylchlorosilane (Thermo Fisher Scientific) were added, followed by a further 30 s of vortexing. Silylation was performed by incubation at 80 °C for a further 120 min. The sample analysis was performed as follows: 1 μl of derivatized sample was injected into a Split/Splitless injector at 200 °C using a 1 in 10 split flow using a Trace GC Ultra gas chromatograph (Thermo Fisher Scientific). Helium carrier

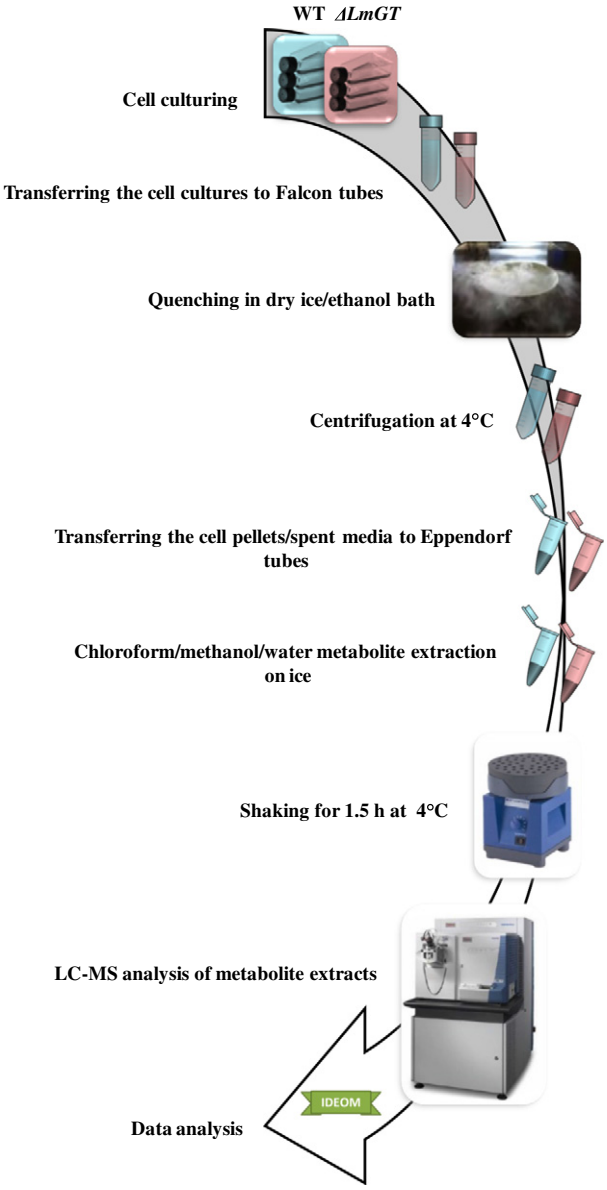

Fig. 1. Workflow of untargeted metabolomic analysis. Abbreviations: WT, wild type parasites; *ΔLmGT*, *ΔLmGT* parasites; LC, liquid chromatography; and MS, mass spectrometry.

gas at a flow rate of 1 ml/min was used for separation on a TraceGOLD TG-5MS GC column, 30 m length × 0.25 mm inner diameter × 0.25 μm film thickness (Thermo Fisher Scientific). The initial oven temperature was held at 40 °C for 1 min, followed by an initial gradient of 33 °C/min ramp to 155 °C. Separation of sugars was performed using a gradient of 10 °C/min from 155 °C to 330 °C with a 1 min final temperature hold at 330 °C. Eluting peaks were transferred through an auxiliary transfer temperature of 250 °C into an ITQ 900 mass spectrometer (Thermo Fisher Scientific). The electron impact ionisation was set to 70 eV energy while the emission current was 250 μA with an ion source of 250 °C. A filament delay of 6 min was used to prevent excess reagents from being ionized. Enhanced selectivity and sensitivity was achieved using selective reaction monitoring (SRM) determined from pure chemical standards for quantitation of metabolites. Fragment ions were isolated using a 2 *m/z* window and excited using collision-induced dissociation (CID). Selected MS2 fragment ion was detected using 6 *m/z* window. Peak detection and quantitation of samples were processed using Xcalibur software (Thermo Fisher Scientific). Calibration curves were calculated using serial dilution of pure standard mixtures with a fixed addition of 1 nmol of ^{13}C-D-glucose. A 7-point calibration curve was then calculated for each compound and this was used to calculate the amount of detected metabolite in the extracted samples. In total, 39 sugars and sugar phosphates were employed as authentic standards to investigate 8 pathways of carbohydrate metabolism.

2.6. Western blotting

Immunoblot analyses were performed using standard sodium dodecyl sulfate-polyacrylamide gel electrophoresis (SDS-PAGE) chemiluminescent procedures, as previously described [16]. To normalize loading, blots were subsequently probed with antisera raised against *L. mexicana* transketolase.

2.7. Scanning electron microscopy

SEM was performed as previously described [19]. Measurements of cell body and flagellar length were made using iTEM software.

2.8. Chemotaxis

Chemotaxis assays were performed as previously described [20], in triplicates, with 100 mM D-glucose as chemoattractant.

3. Results

In order to gain a comprehensive insight into the molecular changes in *Leishmania* parasites in which glucose uptake has been disrupted, we undertook parallel comparative proteomic and metabolomic analyses.

3.1. DiGE analysis of total cellular proteome

Comparative proteomic analysis of biological replicate samples ($n = 4$) revealed that many proteins were reproducibly modulated in *ΔLmGT Leishmania* compared with the wild type parasites and thus confirmed that protein expression is significantly altered in response to loss of glucose uptake capacity (this study and [10,12,13]). 236 protein spots were differentially expressed by <2-fold in all 4 replicates (Fig. 2). We elected, however, to focus on the much smaller number of spots that were differentially expressed by >2-fold ($p \leq 0.05$; $n = 4$) (Fig. 2). Protein matches were obtained for 27 of these spots (Table 1).

3.2. Untargeted analysis of total cellular metabolome

We employed a recently developed metabolite extraction method [17] to perform an untargeted metabolomic analysis and compare biological replicate samples ($n = 3$) of wild type and *ΔLmGT* promastigote cell lysates and spent cell culture media (Fig. 1). The data were analysed with the IDEOM software [18] which was used to perform a Principal Component Analysis (PCA) and a global metabolomic analysis. The PCA analysis illustrated distinct grouping of wild type and *ΔLmGT* cell and spent medium samples (Fig. 3). The comparative metabolomic analysis resulted in the annotation of 799 metabolites, 79 of which showed statistically significant differences ($p < 0.05$; ≥2-fold) in the parasite lysates and 43 in the spent media. 10 of the cellular metabolites (Table 2) and 6 of the secreted metabolites were identified through comparison with authentic standards. The remainder were putatively identified based on accurate mass (±2 ppm) and predicted retention time [18]. Three major categories of metabolites were represented in the promastigote lysate and spent medium samples: metabolites of lipid and amino acid metabolism and metabolites with unassigned biochemical origin (Fig. 4). The lipids were excluded from this investigation because all, except phosphocholine and phosphoethanolamine, were putatively identified on the basis of mass measurements, without any structural analysis to resolve isomers. Furthermore, global lipidomic comparison between wild type and *ΔLmGT* parasites revealed a

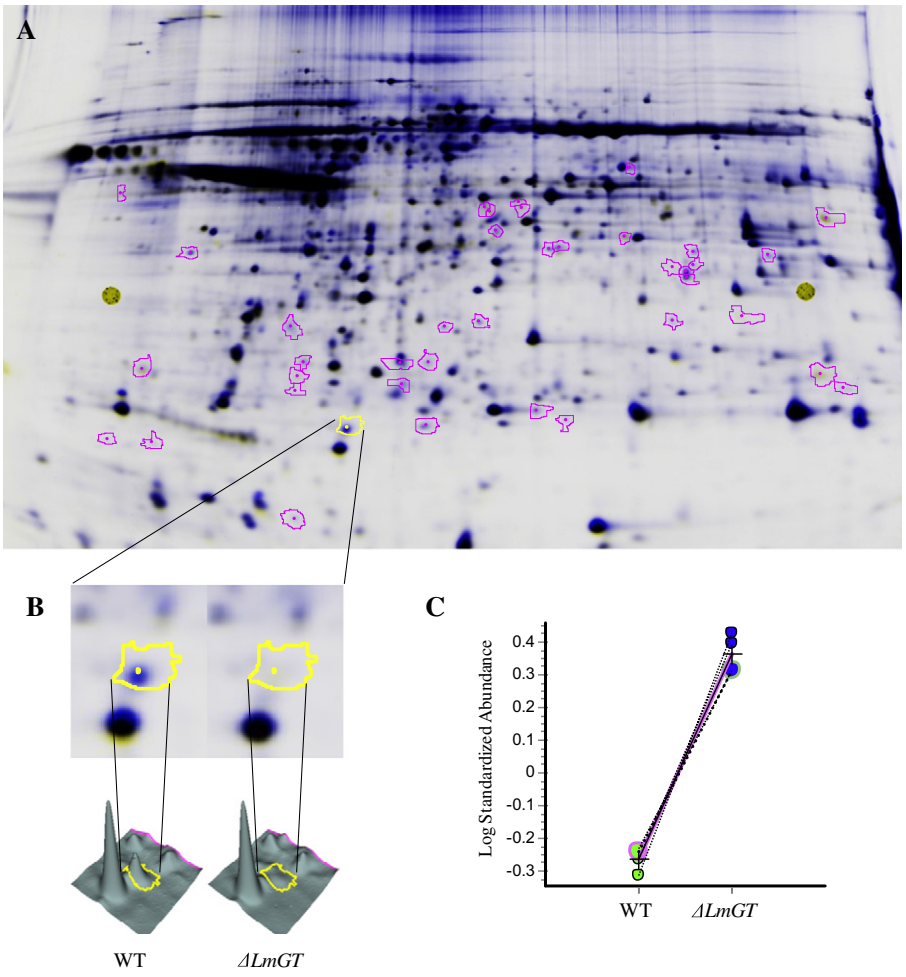

Fig. 2. 2D DiGE analysis of wild type and *ΔLmGT* promastigotes. (A) Representative DiGE overlay image of wild type (yellow) and *ΔLmGT* (blue) proteins. Circled in pink are the spots analysed by mass spectrometry. (B) Overlay image of spot no. 2108 illustrating decreased expression of the corresponding protein in the *ΔLmGT* promastigotes (right panels). (C) Standardized abundance of the protein corresponding to spot no. 2108 in all 4 replicates. Abbreviations: WT, wild type parasites; *ΔLmGT*, *ΔLmGT* parasites.

considerable number of non-significant but a minimal number of significant changes to lipid metabolism in *ΔLmGT Leishmania* (data not included). Additionally, peptides and metabolites with unassigned origin were also excluded from the lists of putatively identified metabolites.

3.3. Targeted analysis of carbohydrates

GC–MS analysis was performed to elucidate alterations in central pathways of carbohydrate metabolism, including glycolysis/gluconeogenesis, pentose phosphate pathway (PPP), and inositol phosphate metabolism (Tables 3 and 4).

The results of the proteomic and metabolomic comparisons are presented together, to facilitate integrated interpretation of the observed changes in *ΔLmGT Leishmania*.

3.4. Carbohydrate metabolism is down-regulated in ΔLmGT Leishmania

As predicted, the omic data revealed that carbohydrate metabolism is significantly modulated in the *ΔLmGT* parasites.

3.4.1. Glycolysis/gluconeogenesis

As speculated previously [12], the inability of *ΔLmGT Leishmania* to utilize exogenous glucose leads to a distinct shift in the glycolytic/gluconeogenic flux. One of the most striking changes we observed was an increase in abundance of a hexose sugar in *ΔLmGT* parasites. This metabolite was chromatographically distinct from fructose, mannose, and galactose and behaved identically to the authentic standard for glucose in the GC–MS analysis. In contrast to glucose, several glycolytic/gluconeogenic intermediates showed decreased levels in *ΔLmGT Leishmania* compared with the wild type parasites (Table 3). Importantly, the level of fructose 1,6-bisphosphate (*F*1,6B) was reduced to below the level of detection in *ΔLmGT*, consistent with the inhibition of phosphofructokinase (PFK) and activation of fructose bisphosphatase (FBP) that would switch metabolic flux from glycolysis to gluconeogenesis.

The proteomic analysis showed that glyceraldehyde 3-phosphate dehydrogenase (GAPDH) was up-regulated in the *ΔLmGT* parasites (Table 1). Under the action of GAPDH, glyceraldehyde 3-phosphate (GAP) is converted to glycerate 1,3-bisphosphate with the simultaneous reduction of NAD^+ to NADH, which must be re-oxidized to maintain the glycosomal NAD^+/NADH balance. In glucose-replete conditions, glycosomal succinate fermentation is the primary mechanism by which *Leishmania* maintains this balance, with an insignificant contribution from the dihydroxyacetone phosphate/glycerol 3-phosphate (DHAP/G3P) shuttle [21]. In *ΔLmGT Leishmania*, however, the intracellular level of succinate is significantly (>5-fold) decreased while that of glycerol is highly (>10-fold) increased (Table 2), suggesting that glycerol is both used as a glucogenic precursor [12] and consumed in the DHAP/G3P shuttle which appears to play a greater role in the regeneration of NAD^+ when gluconeogenesis is active.

3.4.2. Pentose phosphate pathway (PPP)

Decreased levels of 6-phosphogluconate (6PGl) and ribulose 5-phosphate (Ru5P) in the *ΔLmGT* parasites (Table 3) suggest that the oxidative phase of PPP is decreased and imply that the level of NADPH is

Table 1
Protein spots highlighted by DiGE analysis and identified by mass spectrometry.

Accession number	Putative protein	Av. ratio (WT/*ΔLmGT*)	*t*-Test ($n = 4$)	MOWSE score
LmxM.15.1040	Tryparedoxin peroxidase	−13.25	0.00000076	278
LmxM.23.0040	Peroxidoxin, tryparedoxin peroxidase	−6.8	5.20E−05	214
LmxM.23.0110	GDP-mannose pyrophosphorylase	−5.66	0.0000078	228
LmxM.31.1580	Phosphomannose isomerase	−5.17	8.00E−06	165
LmxM.23.0110	GDP-mannose pyrophosphorylase	−3.77	0.000024	258
LmxM.36.0180	Elongation factor 2	−3.7	0.00067	409
LmxM.14.1360	myo-Inositol-1-phosphate synthase	−3.48	0.0000078	398
LmxM.14.1160	Enolase	−3.13	0.0001	1135
LmxM.28.2910	Glutamate dehydrogenase, putative	−3.12	2.60E−06	206
LmxM.29.3360	Calmodulin-related protein, putative	−2.66	0.0023	105
LmxM.29.2980	Glyceraldehyde 3-phosphate dehydrogenase, glycosomal	2.75	2.70E−05	390
LmxM.25.1120	Aldehyde dehydrogenase, mitochondrial precursor	2.82	0.0026	103
LmxM.13.0090	Carboxypeptidase, metallo-peptidase, Clan MA(E), family 32	3.1	0.00019	199
LmxM.18.1580	Non-specific nucleoside hydrolase	3.19	0.00035	106
LmxM.34.0050	2-Oxoisovalerate dehydrogenase β subunit, mitochondrial precursor	3.27	0.0072	157
LmxM.29.2980	Glyceraldehyde 3-phosphate dehydrogenase, glycosomal	3.34	2.10E−05	175
LmxM.31.1000	Chaperonin containing T-complex protein, putative	3.67	0.0031	229
LmxM.18.0210	Hypothetical protein, conserved	4.09	5.80E−05	240
LmxM.29.0735	Co-chaperone, GrpE, putative, heat shock protein GrpE	4.15	2.70E−05	247
LmxM.11.0960	40S ribosomal protein S5	4.23	1.70E−06	121
LmxM.36.2030	Chaperonin HSP60, mitochondrial precursor	4.73	1.30E−06	152
LmxM.16.1430	Paraflagellar rod protein 2C	6.12	0.000025	852
LmxM.16.1430	Paraflagellar rod protein 2C	6.31	0.0000035	1057
LmxM.16.1430	Paraflagellar rod protein 2C	6.97	0.0000035	864
LmxM.32.0312	Heat shock protein 83	10.46	0.0000013	796
LmxM.26.1570	Thimet oligopeptidase, putative, metallo-peptidase, Clan MA(E), Family M3	10.46	0.0000013	174
LmxM.26.1240	Heat shock protein 70-related protein	13.34	1.80E−06	305

most probably also decreased, which would lead to dysregulation of the glycosomal NADPH/NADP ratio and, potentially, the intracellular redox balance. The majority of intermediates of the non-oxidative phase were also decreased in *ΔLmGT*. The level of ribose, notwithstanding, was increased (Table 3). *ΔLmGT* parasites are unable to scavenge this pentose from the environment [22], suggesting that it must be synthesized intracellularly. The increased level of ribose and the up-regulation of a non-specific nucleoside hydrolase (Table 1), together with the previously reported up-regulation of ribokinase in *ΔLmGT* [23], points toward a mechanism for recycling of ribose from nucleotide metabolism.

3.4.3. Fructose and mannose metabolism

Fructose, sucrose, sorbitol and ribitol were increased in the *ΔLmGT* parasites (Table 3). Sucrose, which can be acquired by a sucrose/H^+ transport system [24] and hydrolysed by a sucrase [25] in *Leishmania*, is a source of glucose and fructose. Similarly, sorbitol could be a source of fructose 6-phosphate (F6P) while ribitol, through Ru5P, could be converted to ribose 5-phosphate (R5P). In *Leishmania*, F6P is used in the synthesis of an array of biopolymers. First, under the action of phosphomannose isomerase (PMI), F6P is converted to M6P. PMI was found down-regulated by 5-fold in *ΔLmGT Leishmania* (Table 1). Additionally, two isoforms of GDP-mannose pyrophosphorylase (GDPMP) (LmxM.23.0110), which catalyses the production of GDP-mannose (GDP-Man), the activated mannose donor for all glycosylation reactions, were down-regulated, by 4-fold and 6-fold, in the *ΔLmGT* parasites. The reduced expression of these enzymes would thus decrease the flux from the hexose pool into several major anabolic pathways, including glycoconjugate, lipid anchor, and β-mannan biosynthesis.

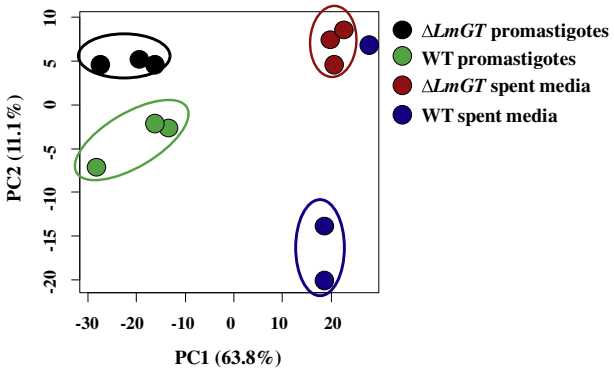

Fig. 3. Principal component analysis (PCA) of metabolomic datasets collected from cell lysate and spent cell culture medium of wild type and *ΔLmGT* promastigotes. Abbreviations: WT, wild type parasites; *ΔLmGT*, *ΔLmGT* parasites.

3.4.4. Inositol phosphate metabolism

Both *myo*-inositol and *myo*-inositol 1-phosphate have approximately 3-fold higher levels in *ΔLmGT Leishmania* compared with the wild type parasites (Table 3). At the same time, *myo*-inositol 1-phosphate synthase, which mediates the first step in the synthesis of all inositol compounds, was down-regulated by 4-fold (Table 1), suggesting that G6P is not diverted toward inositol biosynthesis, and that the higher levels of *myo*-inositol and *myo*-inositol 1-phosphate in *ΔLmGT Leishmania* therefore result from phospholipid breakdown.

3.5. Amino acid utilization is increased in ΔLmGT Leishmania

Beside carbohydrates, amino acids and lipids are potential energy sources for the *Leishmania* parasites [4,26–28]. Our lipidomic analysis revealed that lipid metabolism was not significantly affected by the absence of glucose uptake in the *ΔLmGT* parasites. This observation was not unexpected considering that *Leishmania* are able to acquire needed fatty acids from the environment [26] but do not possess the enzymatic capacity to use them as glucogenic precursors [29]. The untargeted metabolomic analysis, on the other hand, showed that amino acid metabolism is significantly modulated in the *ΔLmGT Leishmania* and confirmed that these parasites relied mainly on amino acids for gluconeogenesis. Indeed, major glucogenic amino acids such as alanine, aspartate, glutamate and proline had considerably decreased levels in the *ΔLmGT* parasites (Table 5). The level of proline, in particular, was even greatly decreased in the spent media which is consistent with rapid uptake and metabolism by *ΔLmGT Leishmania*.

Table 2
Significantly modulated metabolites in *ΔLmGT* parasites, with annotation confidence assigned by IDEOM.

Mass	Formula	Isomers	Putative metabolite	Confidence	Pathway	Av. ratio (WT/*ΔLmGT*)	*t*-test ($n = 3$)
92.05	$C_3H_8O_3$	1	Glycerol	8	Glycerolipid metabolism	14.38	0.015582
123.03	$C_6H_5NO_2$	4	Nicotinate	10	Nicotinate and nicotinamide metabolism	9.21	0.005055
141.02	$C_2H_8NO_4P$	2	Phosphoethanol-amine	10	Glycerophospholipid metabolism; sphingolipid metabolism	9.14	0.034418
131.06	$C_5H_9NO_3$	14	Glutamate 5-semialdehyde	8	Arginine and proline metabolism	3.41	0.021528
400.1	$C_{14}H_{20}N_6O_4S_2$	1	Ovothiol A disulfide	5	Redox metabolism	3.31	0.014403
111.04	$C_4H_5N_3O$	1	Cytosine	10	Pyrimidine metabolism	3.13	0.00039
183.07	$C_5H_{14}NO_4P$	1	Phosphocholine	10	Glycerophospholipid metabolism	2.35	0.02897
117.08	$C_5H_{11}NO_2$	17	Betaine	10	Glycine, serine and threonine metabolism	2.26	0.007684
145.04	$C_5H_7NO_4$	2	2-Oxoglutaramate	8	Glutamate metabolism	2.16	0.002722
158.03	$C_5H_6N_2O_4$	3	Dihydroorotate	8	Pyrimidine metabolism	−2.44	0.011633
134.06	$C_5H_{10}O_4$	8	Deoxyribose	8	Pentose phosphate pathway	−2.70	0.007771
147.05	$C_5H_9NO_4$	14	L-Glutamate	10	Arginine, glutamate and proline metabolism; glutathione metabolism	−3.12	0.002828
133.04	$C_4H_7NO_4$	4	L-Aspartate	10	Alanine and aspartate metabolism; arginine and proline metabolism	−3.22	4.71E−06
89.048	$C_3H_7NO_2$	9	L-Alanine	10	Alanine and aspartate metabolism	−4.54	3.92E−05
307.08	$C_{10}H_{17}N_3O_6S$	3	Glutathione	10	Glutathione metabolism	−6.67	0.042078
118.03	$C_4H_6O_4$	7	Succinate	10	TCA cycle; oxidative phosphorylation	−9.09	0.021543

3.6. Redox metabolism is down-regulated in ΔLmGT Leishmania

A number of enzymes of trypanothione metabolism, with key roles in defense against oxidative stress, were differentially expressed in the *ΔLmGT* parasites. Proteomic comparisons revealed that tryparedoxin peroxidase was consistently down-regulated by approximately 13-fold in *ΔLmGT Leishmania* (Table 1), and this down-regulation was confirmed by Western blotting with a polyclonal antisera raised against *L. major* tryparedoxin peroxidase (Fig. 5). Peroxidoxin, a homologue of tryparedoxin peroxidase, was also strongly down-regulated in the *ΔLmGT* parasites (Table 1). These peroxidases are responsible for maintaining low molecular weight thiols such as glutathione, glutathionylspermidine, trypanothione, and ovothiol in a reduced state. Metabolomic analysis revealed that ovothiol A disulfide levels were 3-fold increased in *ΔLmGT* parasites while levels of glutathione were 6-fold lower (Table 2). Although the glutathione conjugates glutathionylspermidine and trypanothione were not detected, the decreased levels of key precursors such as glutamate and glutathione suggest that trypanothione synthesis (Fig. 6) is most probably suppressed in the *ΔLmGT* parasites.

3.7. Non-metabolic alterations in ΔLmGT Leishmania

Evident from the proteomic data was that metabolic enzymes constituted a large portion of the differentially expressed proteins in the *ΔLmGT* parasites (Table 1). Equally pronounced in these organisms, however, were also a number of non-metabolic proteomic changes, including the up-regulation of heat shock proteins and components of the proteasome and the paraflagellar rod (Table 1). A cluster of strongly expressed protein spots that are encoded by paraflagellar rod 2C (PFR 2C; LmxM.16.1430) was a prominent feature on 2D gels maps of the *L. mexicana* promastigote proteome. These protein spots were co-ordinately up-regulated by approximately 6-fold in the *ΔLmGT* parasites, suggesting a major change in the composition or turnover of the paraflagellar rod, and prompting us to investigate possible changes in flagellar structure and function. The average flagellum length, measured from scanning electron microscopy images, was significantly greater, by approximately 20%, in the *ΔLmGT* parasites (Fig. 7A). We compared the migration of wild type and *ΔLmGT* parasites toward glucose, using an assay we have previously reported [20] and found that, while wild

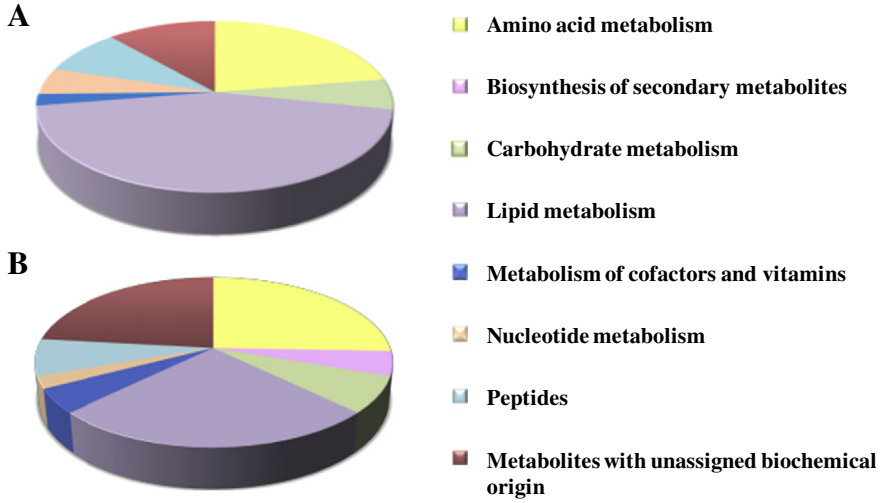

Fig. 4. Distribution of significantly modulated metabolites in *ΔLmGT* parasites. Pie charts illustrate the metabolic role of significantly modulated metabolites in the *ΔLmGT* parasites (A) and spent cell culture media (B).

Table 3
Comparison of carbohydrates in wild type and *ΔLmGT* parasites. Levels of 39 carbohydrates available as authentic standards were measured in cell lysates, and in fresh culture medium. Specified in pink are metabolites of glycolysis/gluconeogenesis; in blue, metabolites of fructose and mannose metabolism; in green, metabolites of galactose metabolism; in violet, metabolites of pentose phosphate pathway; in orange, metabolites of pentose and glucuronate interconversions; in yellow, metabolites of inositol phosphate metabolism; in grey, metabolites of starch and sucrose metabolism; and in white, metabolites belonging to no pathway. All values are in nanomoles/10^8 cells. Abbreviations: iFBS, heat-inactivated fetal bovine serum; NF, not found. No asterisk, a mean of three values; **, a mean of two values; *, an individual value.

Metabolite	Concentration, nM (mean±SD)		
	HOMEM + 10% iFBS (n = 3)	WT (n = 3)	*ΔLmGT* (n = 3)
Glucose	261 ± 94	0.94 ± 0.06	12 ± 4
Glucose 6-phosphate	NF	615 ± 38	150 ± 19
Fructose 6-phosphate	NF	1000 ± 500	369 ± 154*
Fructose 1,6-bisphosphate	617 ± 15*	647 ± 15*	NF
Glyceraldehyde 3-phosphate	NF	NF	NF
Dihydroxyacetone phosphate	NF	1700 ± 600	NF
2-Phosphoglycerate	301 ± 172	4300 ± 2500	4200 ± 1900
Phosphoenolpyruvate	35 ± 0.0**	7700 ± 5900	7100 ± 3500
Fructose	0.24 ± 0.06	0.007 ± 0.006	0.35 ± 0.13
Fructose 1-phosphate	NF	211 ± 0.0**	NF
Mannose	0.78 ± 0.05	NF	NF
Mannose 6-phosphate	NF	NF	NF
Sorbitol	1.2 ± 0.3	5.5 ± 1.1	66 ± 27
Mannitol	0.27 ± 0.14	NF	NF
Rhamnose	NF	NF	NF
Fucose	NF	NF	NF
Galactose	NF	NF	NF
Galactitol	NF	NF	NF
Raffinose	NF	NF	NF
Lactose	NF	NF	NF
6-Phosphogluconate	0.54 ± 0.014*	507 ± 155	398 ± 0.00**
Ribulose 5-phosphate	NF	521 ± 174	NF
Ribose 5-phosphate	NF	1500 ± 600	521 ± 260*
Ribose	0.06 ± 0.001*	0.087 ± 0.0**	0.28 ± 0.013
2-Deoxyribose	NF	NF	NF
Erythrose 4-phosphate	1000 ± 500	NF	3400 ± 2000
Sedoheptulose 7-phosphate	NF	276 ± 4.8	62 ± 27 *
Xylo se	NF	NF	NF
Xylulose	0.009 ± 0.001	NF	NF
Xylitol	0.026 ± 0.013	0.45 ± 0.11	0.35 ± 0.17
Arabinose	0.007 ± 0.0	0.46 ± 0.25	0.07 ± 0.05*
Ribitol	0.04 ± 0.013	0.56 ± 0.3	1.4 ± 0.0**
myo-Inositol	4.3 ± 0.2	133 ± 39	350 ± 139
myo-Inositol 1-phosphate	NF	0.042 ± 0.02	0.150 ± 0.65
Sucrose	0.027 ± 0.002	0.03 ± 0.02	0.093 ± 0.052
Maltose	NF	NF	NF
Threose	0.2 ± 0.0*	0.82 ± 0.35*	1.1 ± 0.00**
Erythrose	NF	NF	NF
2-Deoxyglucose	NF	NF	NF

Table 4
Comparison of carbohydrates in wild type and *ΔLmGT* spent culture media. Levels of 39 carbohydrates available as authentic standards were measured in spent culture medium, and in fresh culture medium. Specified in pink are metabolites of glycolysis/gluconeogenesis; in blue, metabolites of fructose and mannose metabolism; in green, metabolites of galactose metabolism; in violet, metabolites of pentose phosphate pathway; in orange, metabolites of pentose and glucuronate interconversions; in yellow, metabolites of inositol phosphate metabolism; in grey, metabolites of starch and sucrose metabolism; and in white, metabolites belonging to no pathway. All values are in nanomoles/10^8 cells. Abbreviations: iFBS, heat-inactivated fetal bovine serum; NF, not found. No asterisk, a mean of three values; **, a mean of two values; *, an individual value.

Metabolite	Concentration, nM (mean±SD)		
	HOMEM + 10% iFBS (n = 3)	WT (n = 3)	*ΔLmGT* (n = 3)
Glucose	261 ± 94	122 ± 22	211 ± 17
Glucose 6-phosphate	NF	NF	NF
Fructose 6-phosphate	NF	4 ± 0.0**	NF
Fructose 1,6-bisphosphate	617 ± 15**	NF	NF
Glyceraldehyde 3-phosphate	NF	NF	NF
Dihydroxyacetone phosphate	NF	NF	NF
2-Phosphoglycerate	301 ± 172	392 ± 0.0**	156 ± 0.0**
Phosphoenolpyruvate	35 ± 0.0*	NF	NF
Fructose	0.24 ± 0.06	0.22 ± 0.02	0.19 ± 0.005
Fructose 1-phosphate	NF	NF	NF
Mannose	0.78 ± 0.05	0.72 ± 0.02	0.72 ± 0.02
Mannose 6-phosphate	NF	NF	NF
Sorbitol	1.2 ± 0.3	1 ± 0.11	0.99 ± 0.05
Mannitol	0.27 ± 0.14	0.24 ± 0.0**	0.17 ± 0.003
Rhamnose	NF	NF	NF
Fucose	NF	NF	NF
Galactose	NF	NF	NF
Galactitol	NF	NF	NF
Raffinose	NF	NF	NF
Lactose	NF	NF	NF
6-Phosphogluconate	0.54 ± 0.014*	1.4 ± 0.4*	NF
Ribulose 5-phosphate	NF	NF	NF
Ribose 5-phosphate	NF	NF	NF
Ribose	0.06 ± 0.001*	0.14 ± 0.001	0.1 ± 0.006
2-Deoxyribose	NF	NF	NF
Erythrose 4-phosphate	1000 ± 500	1100 ± 100	750 ± 100
Sedoheptulose 7-phosphate	NF	NF	NF
Xylose	NF	NF	NF
Xylulose	0.009 ± 0.001	0.046 ± 0.013	0.033 ± 0.0*
Xylitol	0.026 ± 0.013	0.049 ± 0.003*	0.013 ± 0.006*
Arabinose	0.007 ± 0.0	0.017 ± 0.003	0.009 ± 0.005
Ribitol	0.04 ± 0.013	0.05 ± 0.0*	0.03 ± 0.001
myo-Inositol	4.3 ± 0.2	5.2 ± 0.5	3 ± 0.1
myo-Inositol 1-phosphate	NF	185 ± 73	108 ± 27
Sucrose	0.027 ± 0.002	0.055 ± 0.035	0.01 ± 0.002
Maltose	NF	NF	NF
Threose	0.2 ± 0.0**	NF	NF
Erythrose	NF	NF	NF
2-Deoxyglucose	NF	NF	NF

type promastigotes showed a clear taxis toward glucose, *ΔLmGT* parasites showed no significant movement toward this sugar (Fig. 7, B).

4. Discussion

Leishmania parasites encounter challenging and contrasting environments as they move through their life cycle. Nutrient availability, among many environmental factors, varies both quantitatively and qualitatively, between hosts. The gut of the sand fly vector, where *Leishmania* promastigotes multiply, is an environment where carbohydrates such as glucose, which represent a major carbon and energy source for the promastigote forms, may be abundant or sparse, according to the diet of the host. However, free sugars are believed to be scarce in the parasitophorous vacuole of mammalian macrophages [3] where the amastigote forms of *Leishmania* develop and display a stringent metabolic response [7]. Promastigotes can thrive in culture without glucose, the likely explanation for the viability of the *ΔLmGT* mutant that is the subject of this study, but sustained glucose limitation, whether imposed by environmental scarcity or loss of uptake capacity, may have consequences for virulence. Selection of the *ΔLmGT* parasites has been associated with other phenotypic and genetic changes that may compensate for the transport lesion under culture conditions but likely have profound consequences for the parasite life cycle. A number of studies have reported phenotypic changes in this mutant, including reduced growth rate [10], reduced synthesis of glycoconjugates [12] and the storage carbohydrate β-mannan [5], reduced infectivity to macrophages [10], and increased sensitivity to oxidative stress [11]. Molecular changes include up-regulation of alternate transporters [13] and amplification of genetic elements [30] and transcriptomic and proteomic analyses have highlighted changes in gene expression that are as yet unexplained [23]. A previous 2D gel-based proteomic comparison of wild type and *ΔLmGT L. mexicana* promastigotes revealed addition protein expression differences [23]. We have integrated published and new proteomic data with our complementary metabolomic analyses, to elucidate a molecular basis for the mutant phenotype.

Table 5
Amino acid levels in wild type and *ΔLmGT* promastigotes and spent culture media. The Spent medium levels of L-aspartate and L-glutamate were not considered because Student's *t*-test showed that they had $p > 0.05$. Abbreviation: *, non-significantly changed.

Amino acid	Intracellular level		Spent medium level	
	Av. ratio (WT/*ΔLmGT*)	*t*-Test ($n = 3$)	Av. ratio (WT/*ΔLmGT*)	*t*-Test ($n = 3$)
L-Alanine	−4.51	0,000039	−3.33	0,023200
L-Aspartate	−3.21	4,71E−06	–	$p > 0.05$
L-Glutamate	−3.12	0,002828	–	$p > 0.05$
L-Proline	−1.85*	0,004173	−2.7	0,029664
L-Arginine, L-asparagine, L-cystine, L-citrulline, L-glutamine, L-histidine, L-lysine, L-methionine, L-ornithine, L-phenylalanine, L-threonine, L-tyrosine, L-serine, and L-valine	Non-significantly changed	–	Non-significantly changed	–

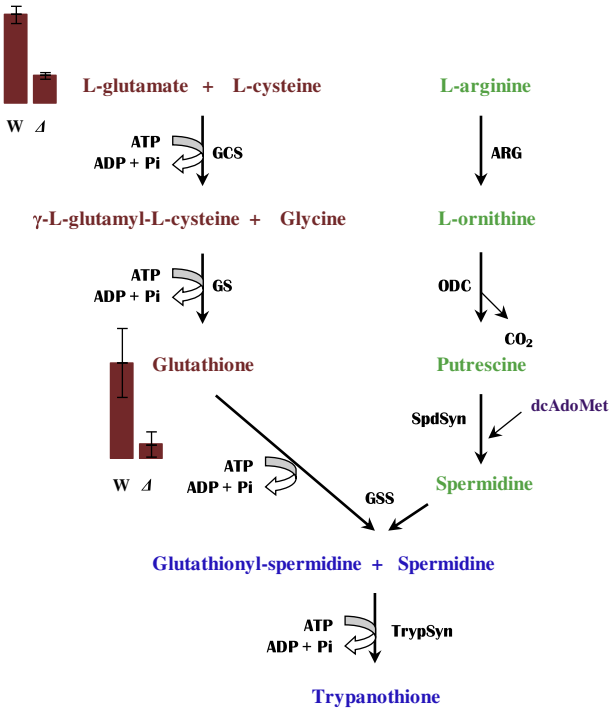

Fig. 6. Trypanothione synthesis. Presented next to L-glutamate and glutathione are histograms depicting their levels in the wild type (W) and *ΔLmGT* (Δ) parasites. Abbreviations: GCS, γ-L-glutamyl-L-cysteine synthetase; GS, glutathione synthase; GSS, glutathionylspermidine synthetase; ARG, arginase; ODC, ornithine decarboxylase; SpdSyn, spermidine synthase; TrypSyn, trypanothione synthase; dcAdoMet, decarboxylated S-adenosyl-L-methionine; ADP, adenosine 5′-diphosphate; ATP, adenosine 5′-triphosphate; Pi, inorganic phosphate; W, wild type parasites; Δ, *ΔLmGT* parasites.

4.1. *ΔLmGT Leishmania utilize alternative carbon sources*

The inability of the *ΔLmGT* promastigotes to transport glucose [11] has previously been correlated to a capacity to exploit glucogenic amino acids for the production of glycopolymers and glycoconjugates [12]. We observed that alanine, aspartate and glutamate, in particular, have significantly decreased levels in the *ΔLmGT* parasites while proline is consumed at a higher rate. *Leishmania* encode a plethora of apparent amino acid transporters, the majority of which have not yet been functionally characterized, but none of these have been observed to be up-regulated, either in comparative transcriptomic or proteomic analyses (this study and [23]). However, increased uptake through facilitative membrane transporters may be driven by increased metabolic flux, without a requirement for additional transporter molecules. Conversely, the observation that *ΔLmGT Leishmania* accumulate more free glucose than wild type seems paradoxical but it is possible the mutant is able to acquire glucose across the plasma membrane into the cytosol by an alternative route, as has been demonstrated in suppressor mutants derived from the *ΔLmGT* parasites [13]. This glucose, though acquired a low rate, may accumulate due to the lack of a metabolic sink for free glucose in a mutant that has adapted to rely on gluconeogenesis. Alternatively, this glucose may be unable to access to the glycosome in the *ΔLmGT* mutant, an intriguing possibility given the previously reported up-regulation of the glycosomal HXK in this mutant. However a requirement for a glycosomal glucose transporter is not consistent with the emerging consensus that the glycosomal membrane does not represent a permeability barrier to small molecules [31].

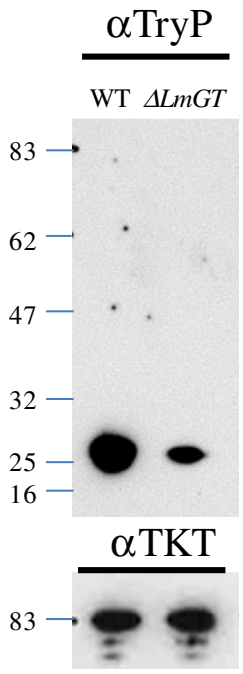

Fig. 5. Western blot with anti-tryparedoxin peroxidase. Abbreviations: TryP, tryparedoxin peroxidase; TKT, transketolase; WT, wild type parasites; *ΔLmGT*, *ΔLmGT* parasites. Numbers indicate apparent molecular weight in kDa.

Alanine, aspartate, glutamate and proline can be exploited as glucogenic precursors by *Leishmania* [21]. Alanine can be converted to pyruvate while aspartate and glutamate can enter the tricarboxylic acid cycle (TCA cycle) through oxaloacetate and α-ketoglutarate, respectively (Fig. 8). Our data further suggest that proline is first oxidized via glutamate 5-semialdehyde (G5S) to glutamate by a proline dehydrogenase and a Δ^1-pyrroline-5-carboxylate dehydrogenase [32], and then metabolized via α-ketoglutarate [33]. The oxidation of proline to glutamate is an important source of reducing equivalents which are directed toward oxidative phosphorylation for the generation of energy. The observations that glutamate 5-semialdehyde production and proline utilization is increased (Table 2) in *ΔLmGT* parasites suggest that proline is a major carbon source for the *ΔLmGT* parasites, used for both energy and gluconeogenesis. Further confirmation for the use of proline as a glucogenic precursor was gained from a parallel study

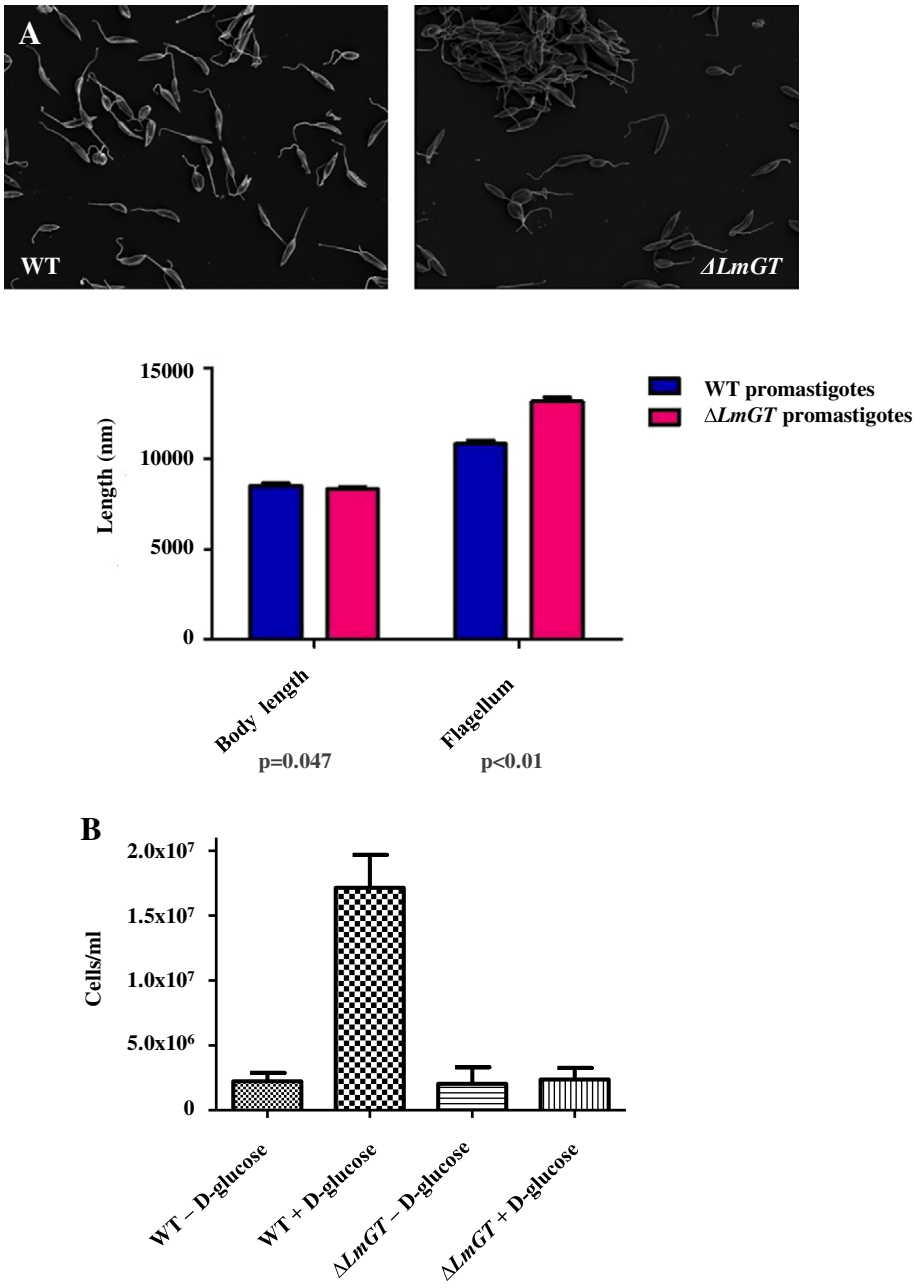

Fig. 7. Analysis of flagellar structure and function of *ΔLmGT* parasites. (A) Scanning electron microscopy images of wild type (WT) and *ΔLmGT* parasites and average measurements of cell body and flagellum from 268 randomly selected WT and *ΔLmGT* cells. A Student's *t*-test indicated a significant difference in average flagellar length ($p \leq 0.001$), but no significant difference in average cell body length ($p = 0.474$). (B) Chemotaxis of WT and *ΔLmGT* promastigotes toward a D-glucose source at 100 mM. Assays were performed in triplicate, with error bars showing standard deviation. Abbreviations: WT, wild type parasites; *ΔLmGT*, *ΔLmGT* parasites; −, without D-glucose; +, with D-glucose.

which showed that both TCA cycle and glycolytic/gluconeogenic intermediates are labelled from ^{13}C-L-proline (manuscript in preparation).

4.2. ΔLmGT Leishmania down-regulate carbohydrate anabolism

Leishmania can utilize gluconeogenesis to synthesize sugar phosphates (Fig. 8), and this is likely the major source of sugars for the *ΔLmGT* parasites. However, the energetic and metabolic constraints associated with gluconeogenesis will limit sugar availability to *ΔLmGT*, compared with wild type parasites that, in culture media, have access to exogenous glucose at mM concentrations. Glucose-6-phosphate (G6P) feeds the pentose phosphate pathway, β-mannan synthesis, the production of a diverse range of glycoconjugates (glycoproteins, lipophosphoglycans, proteophosphoglycans, glycoinositolphospholipids, etc.), and the production of inositols for protein modification, inositol phosphates and lipids. Our observations support the concept that the limited glucose supply is rationed and directed to certain pathways at the expense of others. This has little consequence in rich culture media, but may underpin many of the phenotypes that have been associated with the *ΔLmGT* parasites, and strongly supports the notion that glucose uptake is a potential drug target.

4.2.1. Pentose phosphate pathway

Our data indicate that a significant part of G6P is directed toward the pentose phosphate pathway (PPP) in wild type *Leishmania* (Table 3) but that this is reduced in *ΔLmGT*. As a result, many PPP intermediates have decreased levels in *ΔLmGT*, thus reducing the flow through both the oxidative and non-oxidative phases of the PPP. In the oxidative phase, the

reduced levels of 6-phosphogluconate and ribulose 5-phosphate suggest that the production of NADPH is also decreased. NADPH is an important cofactor in a number of reactions, including the glutamate-α-ketoglutarate interconversion catalysed by a putative cytosolic glutamate dehydrogenase [21], which was 3-fold decreased in the *ΔLmGT* parasites (Table 1), as well as reactions of fatty acid elongation and β-oxidation of fatty acids. NADPH is also involved in defense against oxidative stress via trypanothione. We have observed that trypanothione peroxidase is markedly down-regulated in *ΔLmGT* (Table 1 and Fig. 5), which is more sensitive to oxidative stress [11].

Feng *et al.* [23] have previously reported that the expression of ribokinase is increased in the *ΔLmGT* parasites; an observation that is difficult to reconcile with our observation of increased ribose and reduced ribose-5-phosphate, respectively substrate and product of ribokinase. Ribose uptake, which is mediated by LmGT2, is negligible in *ΔLmGT* [22], suggesting that the ribose we detect must have an

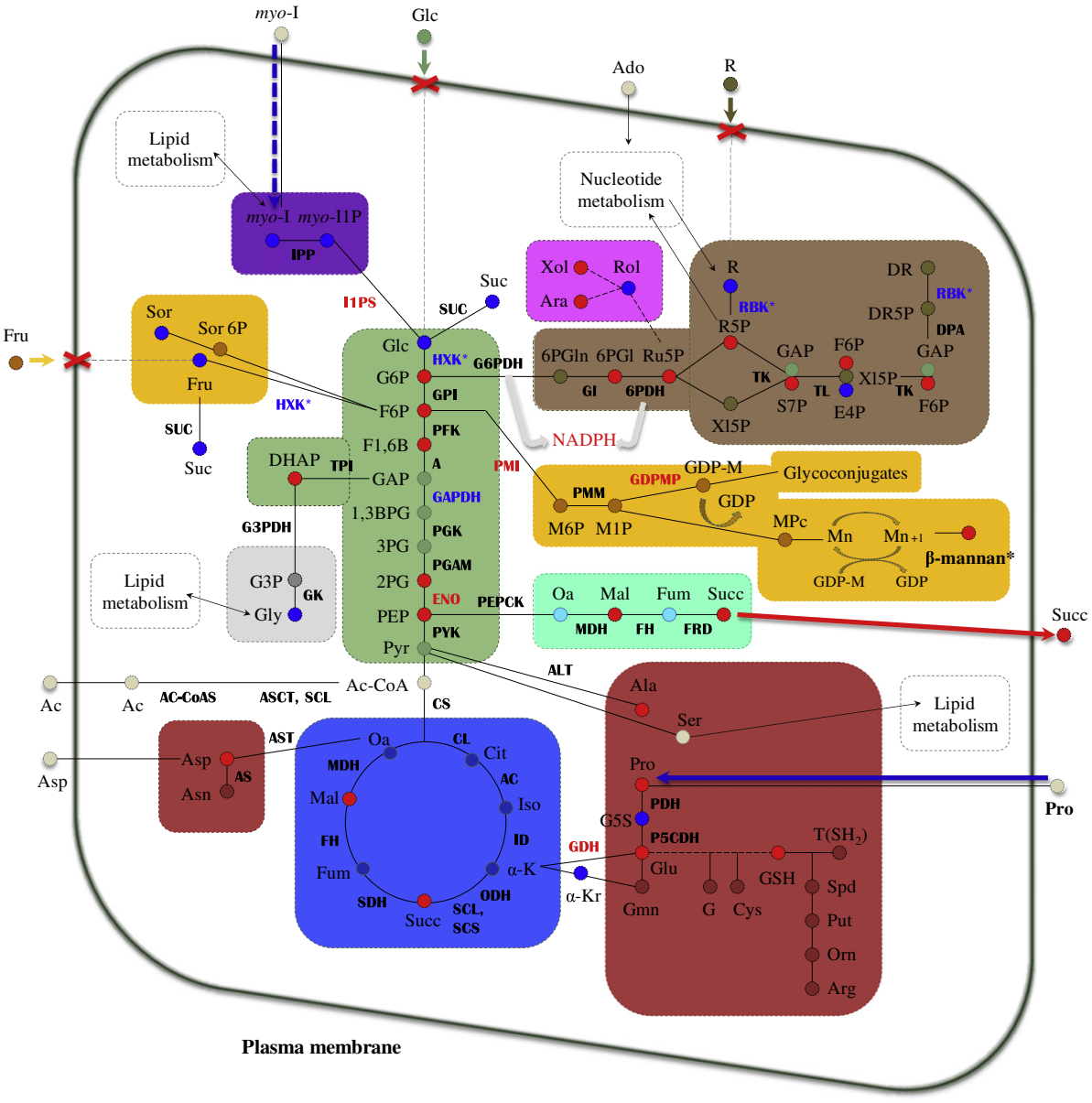

Metabolite with increased level in *ΔLmGT Leishmania*
Metabolite with decreased level in *ΔLmGT Leishmania*
β-mannan* Observed decreased in Rodriguez-Contreras *et al.*, 2006
GAPDH Up-regulated enzyme in *ΔLmGT Leishmania*
HXK* Observed up-regulated in Feng *et al.*, 2011
GDH Down-regulated enzyme in *ΔLmGT Leishmania*
Increased uptake
Decreased secretion
Indirect reaction

Glycolysis/gluconeogenesis
Pentose phosphate pathway
Fructose and mannose metabolism
Inositol phosphate metabolism
Glycerol metabolism
Glycosomal succinate fermentation
Tricarboxylic acid cycle
Amino acid metabolism
Pentose and glucuronate interconversions

endogenous origin. Ribose might be generated through riboneogenesis but sedoheptulose 1,7-bisphosphatase [34] appears to be absent in *Leishmania*, through pentose and glucoronate interconversions from ribitol, which is increased in *ΔLmGT* (Table 3) or by degradation of nucleotides or nucleosides.

4.2.2. Inositol phosphate metabolism

myo-Inositol synthesis involves the consecutive action of an inositol 1-phosphate synthase and an inositol phosphate phosphatase, which together convert G6P to *myo*-inositol. Knockout of *myo*-inositol-1-phosphate synthase in *L. mexicana* gave rise to parasites that were auxotrophic for *myo*-inositol [35]. The observed down-regulation of this enzyme in *ΔLmGT Leishmania* may serve to reduce the proportion of available G6P that is diverted toward the synthesis of phosphatidylinositol precursors. At the same time, *Leishmania* are able to take up *myo*-inositol through a high-affinity *myo*-inosito/H^+ symporter [36] and enhanced import of exogenous *myo*-inositol, abundant in the culture medium (Table 4), may compensate for the reduced biosynthesis in the *ΔLmGT* parasites. Consistent with this possibility, our metabolomic analysis of spent media suggests enhanced uptake of *myo*-inositol by the *ΔLmGT* parasites. In trypanosomes, de novo synthesized and exogenous *myo*-inositol pools are compartmentalized, the former being used for GPI-protein synthesis in the ER and the latter for phosphatidyl inositol lipid synthesis in the Golgi [37]. It is not known if a similar distinction exists in *Leishmania*.

4.2.3. β-Mannan and glycoconjugate synthesis

β-Mannan and glycoconjugate synthesis begins with the activation of mannose to GDP-Man and dolicholphosphate mannose (DP-Man). The enzymes PMI, phosphomannomutase (PMM), GDPMP and dolicholphosphate-mannose synthase (DPMS) are involved in the mannose activation pathway, converting F6P to GDP-Man and DP-Man. The two molecules are the main activated mannose donors in the synthesis of β-mannan and the spectrum of surface associated and secreted glycoconjugates expressed by *Leishmania*, including lipophosphoglycan (LPG), proteophosphoglycans (PPGs), glycosylphosphatidylinositol (GPI)-anchored proteins, glycoinositolphospholipids (GIPLs) and N-glycans [38]. Many of these molecules have been implicated in parasite virulence and, while PMI mutants of *L. mexicana* have decreased glycoconjugate synthesis and virulence [39], a knockout of GDPMP in *L. mexicana* [38] produces parasites that are unable to infect macrophages or animals. Down-regulation of PMI and GDPMP in *ΔLmGT Leishmania* (Fig. 8) may thus contribute to the reduced virulence of this mutant by limiting the flux of sugars into glycoconjugate production.

Key pathways of carbohydrate anabolism are thus down-regulated in *ΔLmGT Leishmania* as a result of reduced glucose flux (Fig. 8). These pathways, however, are likely not required in *Leishmania* promastigotes maintained in axenic culture. Indeed, some of the down-regulated proteins have previously been disrupted in *L. mexicana*, giving rise to parasites that have reduced virulence. The products of these pathways are likely to be important during the in vivo life cycle of the parasites, as they contribute to the synthesis of surface molecules that may modulate host-parasite interactions.

4.3. ΔLmGT Leishmania down-regulate thiol metabolism

Optimal functioning of the PPP pathway, which is a major source of NADPH, is critical for the maintenance of the reduced thiol pool and protection of the organism from oxidative stress. Oxidative stress is a consequence of endogenous metabolism, and the enforced shift from glucose to amino acid catabolism that has occurred in *ΔLmGT Leishmania* may result in complex changes in the type and location of reactive oxygen intermediate (ROI) production within the cell. At the same time, glucose deficit limits flux through the PPP pathway, reducing the pool of NADPH that is the ultimate sink for electrons stripped from ROIs by peroxidases. The most strongly down-regulated protein that we observed in our comparative proteomic analysis was tryparedoxin peroxidase, an observation that we have confirmed by Western blot. Tryparedoxin peroxidase detoxifies hydrogen peroxide and organic peroxides by oxidation of tryparedoxin and other dithiol proteins (Fig. 9). Peroxidoxin, a related protein with a similar function, was also strongly down-regulated. Reduced expression of these enzymes may be an adaptation to glucose limitation that is tolerated in culture because endogenous ROI production is reduced and/or located primarily in the mitochondrion, where amino acids are catabolized. However, the parasite encounters major oxidative challenges in both insect and mammalian hosts and down-regulation of tryparedoxin peroxidase expression will have profound consequences for virulence [16]. Furthermore, we speculate that the increased expression of heat shock proteins and proteasome components reflects increased protein turnover in the *ΔLmGT* mutant, a likely consequence of perturbations to redox homeostasis resulting from down-regulation of tryparedoxin peroxidase and peroxiredoxin.

4.4. ΔLmGT Leishmania promastigotes have altered flagellae and chemotaxis

Comparative proteomic analysis revealed a significant up-regulation of PFR2, one of the two major proteins that comprise the paraflagellar rod in promastigotes. The function of this prominent flagellar structure is enigmatic (reviewed in [40]), but ablation of PFR2 in *L. mexicana* resulted in cells with an aberrant flagellar beat and a loss of forward motility [41]. The substantial (~6 fold) increase in PFR2 expression we observe in *ΔLmGT* points to a change in flagellar biogenesis or structure. Transmission electron microscopy (not shown) revealed no obvious change in the structure of the paraflagellar rod in *ΔLmGT*. However, the increased flagellar length and the loss of a chemotactic response to glucose suggest that flagellar structure and function are altered. It would be of interest to investigate whether other flagellar components are modulated in *ΔLmGT Leishmania* and to explore whether changes in

Fig. 8. Carbon metabolism in *ΔLmGT Leishmania*. Abbreviations: Glc, glucose; G6P, glucose 6-phosphate; F6P, fructose 6-phosphate; *F*1,6B, fructose 1,6-bisphopshate; GAP, glyceraldehydes 3-phosphate; 1,3BPG, 1,3-bisphosphoglycerate; 3PG, 3-phosphoglycerate; 2PG, 2-phosphoglycerate; PEP, phosphoenolpyruvate; Pyr, pyruvate; DHAP, dihydroxyacetone phosphate; G3P, glycerol 3-phosphate; Gly, glycerol; Fru, fructose; Sor, sorbitol; Sor 6P, sorbitol 6-phosphate; Rol, ribitol; Xol, xylito, Ara, arabinose; Ado, adenosine; *myo*-I1P, *myo*-inositol 1-phosphate; *myo*-I, *myo*-inositol; Suc, sucrose; 6PGln, 6-phosphoglucono-1,5-lactone; 6PGl, 6-phosphogluconate; Ru5P, ribulose 5-phosphate; R5P, ribose 5-phosphate; Xl5P, xylulose 5-phosphate; S7P, sedoheptulose 7-phosphate; E4P, erythrose 4-phosphate; R, ribose; DR, 2-deoxyribose; DR5P, 2-deoxyribose 5-phosphate; M6P, mannose 6-phosphate; M1P, mannose 1-phosphate; GDP, guanosine 5′-diphosphate; GDP-Man, guanosine 5′-diphosphate mannose; MPc, mannose 1,4-cyclic-phosphate; Mn, mannan oligomers; Oa, oxaloacetate; Cit, citrate; Iso, isocitrate; α-K, α-ketoglutarate; α-Kr, α-ketoglutaramate; Succ, succinate; Fum, fumarate; Mal, malate; A-CoA, acetyl-CoA; Ac, acetate; Ala, L-alanine; Asp, L-aspartate; Asn, L-asparagine; Arg, L-arginine; Orn, L-ornithine; Put, putrescine; Spd, spermidine; G, glycine; Cys, L-cysteine; Gmn, L-glutamine; Glu, L-glutamate; G5S, glutamate 5-semialdehyde; Pro, L-proline; Ser, L-serine; GSH, glutathione; T(SH)2, trypanothione; NADP, reduced nicotinamide adenine dinucleotide phosphate; HXK, hexokinase; GPI, glucose 6-phosphate isomerase; PFK, phosphofructokinase; A, fructose 1,6-bisphosphate aldolase; GAPDH, glyceraldehyde 3-phosphate dehydrogenase; PGK, phosphoglycerae kinase; PGAM, phosphoglycerate mutase; ENO, enolase; PYK, pyruvate kinase; TPI, triosephosphate isomerase; G3PDH, glycerol 3-phosphate dehydrogenase; GK, glycerol kinase; SUC, sucrase; I1PS, myo-inositol-1-phosphate synthase; IPP, inositol phosphate phosphatase; G6PDH, glucose 6-phosphate dehydrogenase; Gl, gluconolactonase; 6PDH, 6-phosphogluconate dehydrogenase; TK, transketolase; TL, transaldolase; RBK, ribokinase; DPA, deoxyribose-phosphate aldolase; PMI, phosphomannose isomerase; PMM, phosphomannomutase; GDPMP, guanosine 5′-diphosphate mannose pyrophosphorylase; MDH, malate dehydrogenase; FH, fumarate hydratse; FRD, fumarate reductase; ALT, alanine transamminase; CS, citrate synthase; AC-CoAS, acetyl-CoA synthetase; ASCT, acetate:succinate CoA transferase; SCL, succinyl-CoA ligase; AST, aspartate aminotransferase; AS, asparagine synthase; CL, citrate lyase; AC, aconitase; ID, isocitrate dehydrogenase; ODH, 2-oxoglutarate dehydrogenase; SCS, succinyl-CoA synthetase; SDH, succinate dehydrogenase; GDH - glutamate dehydrogenase; PDH, proline dehydrogenase; P5CDH, Δ1-pyrroline-5-carboxylate dehydrogenase.

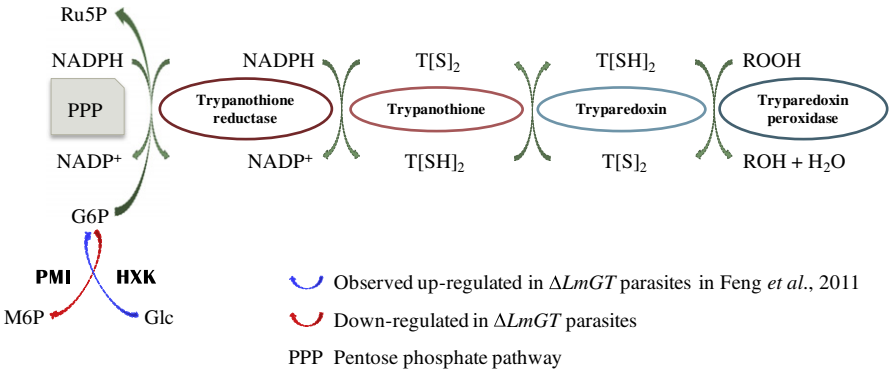

Fig. 9. Schematic of trypanothione metabolism. Abbreviations: NADPH, reduced nicotinamide adenine dinucleotide phosphate; $NADP^+$, oxidized nicotinamide adenine dinucleotide phosphate; $T[S]_2$, trypanothione disulfide; $T[SH]_2$, dihydrotrypanothione; ROOH, hydroperoxides; M6P, mannose-6-phosphate; Glc, glucose; HXK, hexokinase; PMI, phosphomannose isomerase.

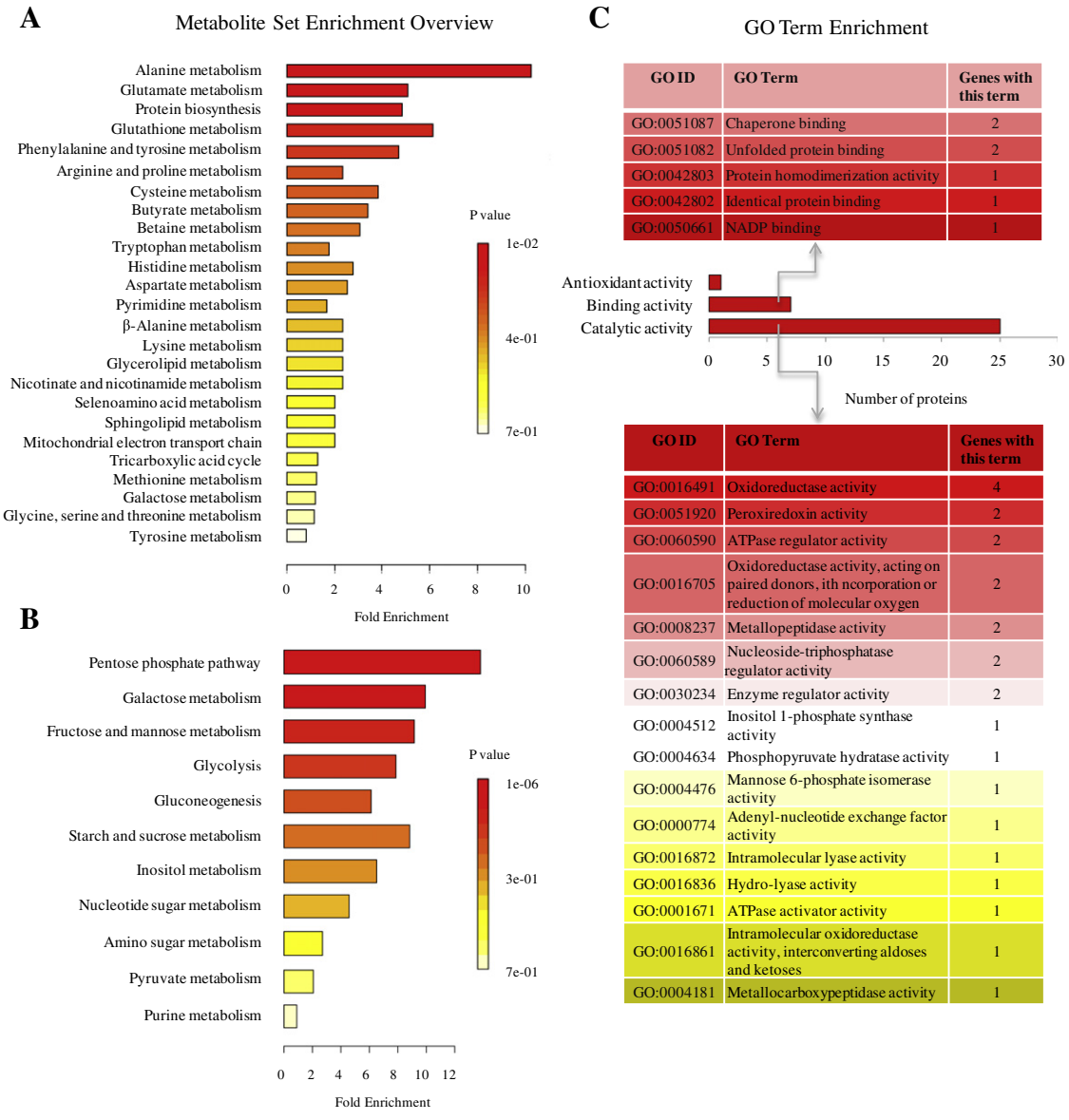

Fig. 10. Bioinformatics analysis of proteomic and metabolomic data. (A) Metabolite Set Enrichment Analysis (MSEA) of modulated intermediates of amino acid metabolism in *ΔLmGT* parasites. (B) MSEA of modulated intermediates of carbohydrate metabolism in *ΔLmGT* parasites. MSEA was performed with MetaboAnalyst (Version 3.0). Considered for the analysis were only (A) the significantly modulated metabolites from the untargeted metabolomic analysis and (B) the modulated sugars and sugar phosphates from the targeted carbohydrate analysis. Lipids, peptides and metabolites with unassigned origin were excluded from the untargeted metabolomic analysis. (C) Gene Ontology Enrichment Analysis (GOEA) of significantly modulated proteins in *ΔLmGT* parasites. GOEA was performed with TritrypDB (Release 28, 31 March 2016). The top table provides a breakdown of the binding activities. The bottom table provides a breakdown of the catalytic activities.

chemotaxis are specific to substrates of the LmGT transporters, one of which (LmGT1) is localized to the flagellum [9], or are more general, suggesting a lesion in directed motility.

4.5. Potential of combined proteomic and metabolomic analyses to elucidate complex phenotypic changes

Integrative investigation of complex biological systems has become more feasible in recent years, as the ability to collect and interpret omic data has increased. However, coverage in such studies remains limited by the complexity, dynamic range and chemical diversity that characterizes both proteome and metabolome. Our data show that the application of orthogonal analytical approaches, such as 2D gel electrophoresis, LC-MS and GC–MS can not only result in more global coverage of biological systems but can also produce complementary datasets that can be interpreted through ontological and correlation analyses.

At the pathway level, the combined data reveal significant changes in amino acid and carbohydrate metabolism (Fig. 10A and B). Reduced expression of pathways that mediate glucose consumption, together with increased expression of alternate nutrient transporters, is a predictable response to a lesion in glucose uptake. However, the modulation in individual pathways of central carbon metabolism, perceived in both proteomic and metabolomic analyses, indicates that the organism has elaborated a complex, system-wide response to the enforced shift in carbon source. Major alternative sources are glucogenic substrates such as amino acids, aided by glycerol, acetate, and some disaccharides and sugar alcohols. Hexose phosphates are generated in limited amounts by gluconeogenesis and are then rationed between various pathways. The pentose phosphate pathway, deprived of both exogenous glucose and ribose, is sustained at a reduced level by glucose-6-phosphate of gluconeogenic origin, and potentially by ribose scavenged from nucleotide metabolism. The latter appears to be only moderately affected by the carbon source shift due to the existance of multiple acquisition and biosynthetic routes for nucleotides, nucleosides or nucleic acids in *Leishmania* [42]. Production of glycoconjugates and carbohydrate reserves is down-regulated, apparently by reduced expression of key feeder enzymes.

At the system level, our integrated analysis reveals extensive remodelling of *Leishmania* metabolism, and implies the existence of mechanisms that coordinate these changes. Reorganization of cellular structure, remodelling of carbon source dependence, increased protein turnover, decreased anabolism and reduced oxidative defense constitute the main changes in *ΔLmGT* metabolism. These appear to be coordinated through control of substrate utilization, proteostasis, and redox and ATP metabolism (Fig. 10). Systematic modulation of protein synthesis, processing and degradation (evidenced by the up-regulation of protein chaperones (Fig. 10C)) and production, utilization and exchange of NAD and ATP may reflect adaptations in the *Leishmania* life cycle that maintain cellular homeostasis in the face of a changing environment. We postulate that this programmed remodelling of substrate acquisition and metabolism may have been called into play during the selection of the *ΔLmGT* mutant. In a rich culture medium, all of these adaptations may be tolerable but the persistent metabolic and environmental stress that is encountered throughout the life cycle may compromise parasite survival, providing an explanation for the increased sensitivity to oxidative stress and reduced virulence that has been reported for this mutant. The major changes we observed in expression of paraflagellar rod proteins, which led us to obtain evidence of changes in flagellar structure and function, may also be related to life cycle switching and warrant further study. While this study cannot be extended to amastigote forms, as the *ΔLmGT* mutant does not replicate as this stage, the application of proteomic and metabolomic analysis to *Leishmania* amastigotes has great potential to increase understanding of metabolism in the clinically relevant stage.

Abbreviations

2D	two dimensional
6PGl	6-phosphogluconate
ACN	acetonitrile
BVA	Batch Variance Analysis
CID	collision-induced dissociation
DiGE	difference gel electrophoresis
DHAP/G3P shuttle	dihydroxyacetone phosphate/glycerol 3-phosphate shuttle
DP-Man	dolicholphosphate mannose
DPMS	dolicholphosphate-mannose synthase
ESI	electrospray ionisation
*F*1,6B	fructose 1,6-bisphosphate
F6P	fructose 6-phosphate
FA	formic acid
FBP	fructose bisphosphatase
G5S	glutamate 5-semialdehyde
G6P	glucose 6-phosphate
GAP	glyceraldehyde 3-phosphate
GAPDH	glyceraldehyde 3-phosphate dehydrogenase
GC	gas chromatography
GDP	guanosine 5′-diphosphate
GDP-Man	GDP-mannose
GDPMP	GDP-mannose pyrophosphorylase
GIPLs	glycoinositolphospholipids
GPI	glycosylphosphatidylinositol
HOMEM	hemoflagellate-modified minimum essential medium
HXK	hexokinase
iFBS	heat-inactivated fetal bovine serum
iFCS	heat-inactivated fetal calf serum
LC	liquid chromatography
LPG	lipophosphoglycan
MS	mass spectrometry
MSTFA	*N*-methyl-N-(trimethylsilyl) trifluoroacetamide
NAD	nicotinamide adenine dinucleotide
NADP	nicotinamide adenine dinucleotide phosphate
NADPH	reduced nicotinamide adenine dinucleotide phosphate
PBS	phosphate buffer saline
PCA	Principal Component Analysis
PFK	phosphofructokinase
PFR	paraflagellar rod
PMI	phosphomannose isomerase
PMM	phosphomannomutase
PPGs	proteophosphoglycans
PPP	pentose phosphate pathway
ROI	reactive oxygen intermediate
Ru5P	ribulose 5-phosphate
SDS-PAGE	sodium dodecyl sulfate-polyacrylamide gel electrophoresis
SEM	scanning electron microscopy
SRM	selective reaction monitoring
TCA cycle	tricarboxylic acid cycle
TryP	tryparedoxin peroxidise
UHPLC	ultra-high performance liquid chromatography
ZIC-pHILIC	zwitterionic-polymeric hydrophilic interaction chromatography.

Author contributions

S.A., K.B. and R.B. designed the experiments. S.A., S.W., D.L., C.N. and D.H. collected and analysed the data. S.A., M.B. and R.B. wrote the paper.

Funding sources

The work has been partially funded by the Engineering and Physical Sciences Research Council (EPSRC), Grant EP/F500424/1 DTC in Cell and

Proteomic Technologies and by a project grant from the Wellcome Trust, grant number GR075978AIA.

Conflict of interest

The authors declare no competing financial interest.

Transparency document

The Transparency document associated with this article can be found in the online version.

Acknowledgments

We thank Glasgow Polyomics for supporting facilities for proteomic and metabolomics data collection and Alan Scott for the technical assistance with 2D gel electrophoresis. Antisera against tryparedoxin peroxidase were the kind gift of Susan Wyllie.

References

[1] J.J. Blum, Energy metabolism in *Leishmania*, J. Bioenerg. Biomembr. 26 (1994) 147–155.
[2] C.J. Young, D.P. Turner, R. Killick-Kendrick, J.A. Rioux, A.J. Leaney, Fructose in wild-caught *Phlebotomus ariasi* and the possible relevance of sugars taken by sandflies to the transmission of leishmaniasis, Trans. R. Soc. Trop. Med. Hyg. 74 (1980) 363–366.
[3] R.J. Burchmore, M.P. Barrett, Life in vacuoles–nutrient acquisition by *Leishmania* amastigotes, Int. J. Parasitol. 31 (2001) 1311–1320.
[4] D.T. Hart, G.H. Coombs, *Leishmania mexicana*: energy metabolism of amastigotes and promastigotes, Exp. Parasitol. 54 (1982) 397–409.
[5] J.E. Ralton, T. Naderer, H.L. Piraino, T.A. Bashtannyk, J.M. Callaghan, M.J. McConville, Evidence that intracellular beta1-2 mannan is a virulence factor in *Leishmania* parasites, J. Biol. Chem. 278 (2003) 40757–40763.
[6] D. Rodriguez-Contreras, N. Hamilton, Gluconeogenesis in *Leishmania mexicana*: contribution of glycerol kinase, phosphoenolpyruvate carboxykinase, and pyruvate phosphate dikinase, J. Biol. Chem. 289 (2014) 32989–33000.
[7] E. Saunders, W. Ng, J. Kloehn, J. Chambers, M. Ng, M. McConville, Induction of a stringent metabolic response in intracellular stages of *Leishmania mexicana* leads to increased dependence on mitochondrial metabolism, PLoS Pathog. (2014) 10.
[8] R.J. Burchmore, D.T. Hart, Glucose transport in amastigotes and promastigotes of *Leishmania mexicana mexicana*, Mol. Biochem. Parasitol. 74 (1995) 77–86.
[9] R.J. Burchmore, S.M. Landfear, Differential regulation of multiple glucose transporter genes in *Leishmania mexicana*, J. Biol. Chem. 273 (1998) 29118–29126.
[10] R. Burchmore, D. Rodriguez-Contreras, K. McBride, M. Barrett, G. Modi, D. Sacks, S. Landfear, Genetic characterization of glucose transporter function in *Leishmania mexicana*, Proc. Natl. Acad. Sci. U. S. A. 100 (2003) 3901–3906.
[11] D. Rodriguez-Contreras, X. Feng, K.M. Keeney, H.G. Bouwer, S.M. Landfear, Phenotypic characterization of a glucose transporter null mutant in *Leishmania mexicana*, Mol. Biochem. Parasitol. 153 (2007) 9–18.
[12] D. Rodriguez-Contreras, S. Landfear, Metabolic changes in glucose transporter-deficient *Leishmania mexicana* and parasite virulence, J. Biol. Chem. 281 (2006) 20068–20076.
[13] X. Feng, D. Rodriguez-Contreras, C. Buffalo, A. Bouwer, E. Kruvand, S.M. Beverley, S.M. Landfear, Amplification of an alternate transporter gene suppresses the avirulent phenotype of glucose transporter null mutants in *Leishmania mexicana*, Mol. Microbiol. (2008).
[14] R.L. Berens, R. Brun, S.M. Krassner, A simple monophasic medium for axenic culture of hemoflagellates, J. Parasitol. 62 (1976) 360–365.
[15] A. Alban, S.O. David, L. Bjorkesten, C. Andersson, E. Sloge, S. Lewis, I. Currie, A novel experimental design for comparative two-dimensional gel analysis: two-dimensional difference gel electrophoresis incorporating a pooled internal standard, Proteomics 3 (2003) 36–44.
[16] H. Daneshvar, S. Wyllie, S. Phillips, P. Hagan, R. Burchmore, Comparative proteomics profiling of a gentamicin-attenuated *Leishmania infantum* cell line identifies key changes in parasite thiol-redox metabolism, J. Proteome 75 (2012) 1463–1471.
[17] D.P. De Souza, E.C. Saunders, M.J. McConville, V.A. Likic, Progressive peak clustering in GC–MS metabolomic experiments applied to *Leishmania* parasites, Bioinformatics 22 (2006) 1391–1396.
[18] D.J. Creek, A. Jankevics, K.E.V. Burgess, R. Breitling, M.P. Barrett, IDEOM: an Excel interface for analysis of LC–MS-based metabolomics data, Bioinformatics 28 (2012) 1048–1049.
[19] L.S. Morrison, A. Goundry, M.S. Faria, L. Tetley, S.C. Eschenlauer, G.D. Westrop, A. Dostalova, P. Volf, G.H. Coombs, A.P. Lima, J.C. Mottram, Ecotin-like serine peptidase inhibitor ISP1 of *Leishmania* major plays a role in flagellar pocket dynamics and promastigote differentiation, Cell. Microbiol. 14 (2012) 1271–1286.
[20] G. Leslie, M. Barrett, R. Burchmore, *Leishmania mexicana*: promastigotes migrate through osmotic gradients, Exp. Parasitol. 102 (2002) 117–120.
[21] F.R. Opperdoes, G.H. Coombs, Metabolism of *Leishmania*: proven and predicted, Trends Parasitol. 23 (2007) 149–158.
[22] C.M. Naula, F.J. Logan, P.E. Wong, M.P. Barrett, R.J. Burchmore, A glucose transporter can mediate ribose uptake: definition of residues that confer substrate specificity in a sugar transporter, J. Biol. Chem. 285 (2010) 29721–29728.
[23] X. Feng, T. Feistel, C. Buffalo, A. McCormack, E. Kruvand, D. Rodriguez-Contreras, N.S. Akopyants, P.K. Umasankar, L. David, A. Jardim, S.M. Beverley, S.M. Landfear, Remodeling of protein and mRNA expression in *Leishmania mexicana* induced by deletion of glucose transporter genes, Mol. Biochem. Parasitol. 175 (2011) 39–48.
[24] A. Singh, D. Mandal, A novel sucrose/H+ symport system and an intracellular sucrase in *Leishmania donovani*, Int. J. Parasitol. 41 (2011) 817–826.
[25] R.L. Jacobson, Y. Schlein, C.L. Eisenberger, The biological function of sand fly and *Leishmania* glycosidases, Med. Microbiol. Immunol. 190 (2001) 51–55.
[26] J.D. Berman, J.V. Gallalee, J.M. Best, T. Hill, Uptake, distribution, and oxidation of fatty-acids by *Leishmania mexicana* amastigotes, J. Parasitol. 73 (1987) 555–560.
[27] S. Mazareb, Z.Y. Fu, D. Zilberstein, Developmental regulation of proline transport in *Leishmania donovani*, Exp. Parasitol. 91 (1999) 341–348.
[28] M.V. Geraldo, A.M. Silber, C.A. Pereira, S.R.B. Uliana, Characterisation of a developmentally regulated amino acid transporter gene from *Leishmania amazonensis*, FEMS Microbiol. Lett. 242 (2005) 275–280.
[29] A.C. Ivens, C.S. Peacock, E.A. Worthey, L. Murphy, G. Aggarwal, M. Berriman, E. Sisk, M.A. Rajandream, E. Adlem, R. Aert, A. Anupama, Z. Apostolou, P. Attipoe, N. Bason, C. Bauser, A. Beck, S.M. Beverley, G. Bianchettin, K. Borzym, G. Bothe, C.V. Bruschi, M. Collins, E. Cadag, L. Ciarloni, C. Clayton, R.M.R. Coulson, A. Cronin, A.K. Cruz, R.M. Davies, J. De Gaudenzi, D.E. Dobson, A. Duesterhoeft, G. Fazelina, N. Fosker, A.C. Frasch, A. Fraser, M. Fuchs, C. Gabel, A. Goble, A. Goffeau, D. Harris, C. Hertz-Fowler, H. Hilbert, D. Horn, Y.T. Huang, S. Klages, A. Knights, M. Kube, N. Larke, L. Litvin, A. Lord, T. Louie, M. Marra, D. Masuy, K. Matthews, S. Michaeli, J.C. Mottram, S. Muller-Auer, H. Munden, S. Nelson, H. Norbertczak, K. Oliver, S. O'Neil, M. Pentony, T.M. Pohl, C. Price, B. Purnelle, M.A. Quail, E. Rabbinowitsch, R. Reinhardt, M. Rieger, J. Rinta, J. Robben, L. Robertson, J.C. Ruiz, S. Rutter, D. Saunders, M. Schafer, J. Schein, D.C. Schwartz, K. Seeger, A. Seyler, S. Sharp, H. Shin, D. Sivam, R. Squares, S. Squares, V. Tosato, C. Vogt, G. Volckaert, R. Wambutt, T. Warren, H. Wedler, J. Woodward, S.G. Zhou, W. Zimmermann, D.F. Smith, J.M. Blackwell, K.D. Stuart, B. Barrell, P.J. Myler, The genome of the kinetoplastid parasite, *Leishmania major*, Science 309 (2005) 436–442.
[30] X. Feng, D. Rodriguez-Contreras, T. Polley, L.F. Lye, D. Scott, R.J. Burchmore, S.M. Beverley, S.M. Landfear, 'Transient' genetic suppression facilitates generation of hexose transporter null mutants in *Leishmania mexicana*, Mol. Microbiol. (2012).
[31] J.R. Haanstra, E.B. Gonzalez-Marcano, M. Gualdron-Lopez, P.A.M. Michels, Biogenesis, maintenance and dynamics of glycosomes in trypanosomatid parasites, BBA-Mol. Cell. Res. 1863 (2016) 1038–1048.
[32] B.S. Mantilla, L.S. Paes, E.M.F. Pral, D.E. Martil, O.H. Thiemann, P. Fernandez-Silva, E.L. Bastos, A.M. Silber, Role of Delta(1)-pyrroline-5-carboxylate dehydrogenase supports mitochondrial metabolism and host-cell invasion of *Trypanosoma cruzi*, J. Biol. Chem. 290 (2015) 7767–7790.
[33] S.M. Krassner, B. Flory, Proline metabolism in *Leishmania donovani* promastigotes, J. Protozool. 19 (1972) 682–685.
[34] M.F. Clasquin, E. Melamud, A. Singer, J.R. Gooding, X.H. Xu, A.P. Dong, H. Cui, S.R. Campagna, A. Savchenko, A.F. Yakunin, J.D. Rabinowitz, A.A. Caudy, Riboneogenesis in yeast, Cell 145 (2011) 969–980.
[35] T. Ilg, Generation of myo-inositol-auxotrophic *Leishmania mexicana* mutants by targeted replacement of the myo-inositol-1-phosphate synthase gene, Mol. Biochem. Parasitol. 120 (2002) 151–156.
[36] M.E. Drew, C.K. Langford, E.M. Klamo, D.G. Russell, M.P. Kavanaugh, S.M. Landfear, Functional expression of a myo-inositol/H+ symporter from *Leishmania donovani*, Mol. Cell. Biol. 15 (1995) 5508–5515.
[37] A. Gonzalez-Salgado, M.E. Steinmann, E. Greganova, M. Rauch, P. Maser, E. Sigel, P. Butikofer, Myo-inositol uptake is essential for bulk inositol phospholipid but not glycosylphosphatidylinositol synthesis in *Trypanosoma brucei*, J. Biol. Chem. 287 (2012) 13313–13323.
[38] A. Garami, T. Ilg, Disruption of mannose activation in *Leishmania mexicana*: GDP-mannose pyrophosphorylase is required for virulence, but not for viability, EMBO J. 20 (2001) 3657–3666.
[39] A. Garami, T. Ilg, The role of phosphomannose isomerase in *Leishmania mexicana* glycoconjugate synthesis and virulence, J. Biol. Chem. 276 (2001) 6566–6575.
[40] N. Portman, K. Gull, The paraflagellar rod of kinetoplastid parasites: from structure to components and function, Int. J. Parasitol. 40 (2010) 135–148.
[41] C. Santrich, L. Moore, T. Sherwin, P. Bastin, C. Brokaw, K. Gull, J.H. LeBowitz, A motility function for the paraflagellar rod of *Leishmania* parasites revealed by PFR-2 gene knockouts, Mol. Biochem. Parasitol. 90 (1997) 95–109.
[42] N.S. Carter, P. Yates, C.S. Arendt, J.M. Boitz, B. Ullman, Purine and Pyrimidine Metabolism in *Leishmania*, Drug Targets in Kinetoplastid Parasites, 625, 2008 141–154.